

Mesoporous Nickel–Aluminum Mixed Oxide: A Promising Catalyst in Hydride-Transfer Reactions

Manidipa Paul,^[a] Nabanita Pal,^[a] and Asim Bhaumik*^[a]

Keywords: Reduction / Capping agents / Hydrides / Mesoporous materials / Nanostructures

The design and synthesis of a new nanostructured material that can efficiently catalyze selective reduction reactions in an eco-friendly way is an active area of research today. Here a mesoporous Ni–Al mixed oxide material has been synthesized hydrothermally by using lauric acid as capping agent. The mesoporosity observed in the material is mainly originated from the interparticle voids created due to the self-assembly of the nanoparticles (NPs) in the presence of capping agent used during the synthesis. The material has been characterized by powder XRD, N₂ sorption, high-resolution

transmission electron microscopy (HRTEM), scanning electron microscopy/energy-dispersive spectroscopy (SEM-EDS), FTIR, and thermogravimetric/differential thermal analysis (TG-DTA) tools. The mesoporous Ni–Al mixed-oxide material showed a very high Brunauer–Emmett–Teller (BET) surface area (337 m² g⁻¹) and excellent catalytic activity in a selective liquid-phase hydride-transfer reduction reaction of nitroarenes to their corresponding anilines in the presence of 2-propanol as hydride source.

Introduction

Due to their unique properties such as exceptionally high surface areas, uniform and tunable nanoscale pore dimensions, and large pore volumes, mesoporous materials have maintained an outstanding position in the field of materials science since the first report of M41S materials.^[1] With the passage of time and advancements in the field, the attention is now focused on nonsiliceous mesoporous materials, mainly phosphates^[2] and oxides^[3] instead of silica-based organic–inorganic hybrid materials.^[4] Among these materials, mesoporous metal oxides have come to occupy a distinct position owing to their potential application in different frontier areas.^[3] Compared to simple metal oxides, mixed metal oxides such as perovskites^[5] and spinels^[6] have wider scopes because of their tunable structural features through compositional variations and huge potential applications that range from adsorption^[7] and catalysis^[8] to electrode materials.^[9]

Mixed metal oxides that contain transition-metal atoms can play a significant catalytic role in a large variety of heterogeneous chemical processes such as catalytic combustion of hydrocarbons,^[10] CO oxidation,^[11] selective partial oxidation, and reduction of organic molecules.^[12–14] In particular, Ni- and Al-based spinels are potential catalysts in reduction reactions.^[15] In the past, nickel–aluminum spinel oxides have been prepared by diverse synthetic routes through co-precipitation to layered double hydroxides^[16] or

sol–gel^[17] techniques. Tai and Guo have synthesized hexagonal nickel–aluminum oxide by the homogeneous precipitation method.^[18] But the material is amorphous, and its catalytic potential has not been explored. Besides that, the self-organization of nanoparticles (NPs) is another major area of research since it has many practical applications.^[19] Because of their special size, a large number of particles are present at the surface compared to that of the bulk. For this reason, nanostructured materials have found potential utility in a wide range of catalytic reactions.^[20]

In this context it is pertinent to mention that the aromatic amines are an important class of compounds that are used in large-scale industrial processes for the manufacture of dye-stuffs, pharmaceuticals, agrochemicals, photographic chemicals, polymers, chelating agents, and so on. Different methods such as metal/HCl systems, H₂ gas, sulfides and polysulfides, and so forth are commonly utilized as reducing agents for the conversion of nitro compounds to their respective amine derivatives. However, on account of environmental constraints, particular attention has been paid to finding a safer alternative strategy for the reduction of nitro groups in this context. Catalytic hydride-transfer reduction (CHTR) has received significant recognition as an alternative for the clean reduction of a variety of nitroarenes.^[21–23] Several greener processes are available by using a CHTR pathway that utilizes a phase-transfer catalyst,^[21] Zn/ammonium salt/ionic liquid,^[22] ultrasound-promoted reduction,^[23] and so on. But all these methods have limitations with regards to their complex synthetic route and cost-effectiveness. Herein, we report a simple synthetic route for the preparation of mesoporous nickel–aluminum mixed-oxide material through self-assembled NPs in the

[a] Department of Materials Science, Indian Association for the Cultivation of Science, Jadavpur, Kolkata 700032, India
E-mail: msab@iacs.res.in

presence of an anionic template, lauric acid, which plays the role of a capping agent for the positively charged metal cations at the surface of the nanoparticles. Our mesoporous nickel–aluminum oxide material shows a nanocrystalline NiAl_2O_4 spinel structure upon high-temperature calcination. Furthermore, this mesoporous nickel–aluminum oxide shows good regioselectivity in the reduction of nitrobenzenes to anilines in an environmentally safer route by means of hydride transfer from a sacrificial secondary alcohol.

Results and Discussion

Chemical Composition

The chemical composition of the calcined mesoporous nickel–aluminum oxide sample 3 [obtained from energy-dispersive spectroscopy (EDS) analysis] is given in Table 1. The data reveal that the ratio of nickel/aluminum is approximately 0.5 in the sample, although during synthesis of this mesoporous nickel–aluminum oxide we used an Ni/Al molar ratio of 1:1 in the synthesis gel of our first batch. Excess amounts of nickel were leached out during hydrothermal synthesis. Later we used a 1:2 molar ratio of Ni/Al in the synthesis batch, and the final product also followed a similar chemical composition. An excess amount of O (Table 1) could be attributed to the surface defects and the presence of adsorbed water molecules. Thus, the chemical formula for our mesoporous nickel–aluminum oxide can be written as $\text{NiO–Al}_2\text{O}_3$.

Table 1. EDS results for the mesoporous Ni–Al oxide sample 3 calcined at 773 K.

Element	[keV]	Mass-%	Atom-%
Ni K	7.471	23.14	8.48
Al K	1.486	21.58	17.2
O K	0.525	55.29	74.32
Total		100.00	100.00

Characterizations

Powder XRD

The wide-angle powder XRD patterns of the mesoporous nickel–aluminum oxide samples calcined at 773 and 1073 K are shown in Figure 1. It is interesting to note that no peak for either nickel or nickel oxide (NiO) is observed for the sample calcined at 773 K. This pattern is similar to the XRD pattern of alumina (Al_2O_3). This anomaly arises at this stage due to the fact that the Ni^{II} sites remain highly dispersed in the mesoporous alumina matrix,^[24,25] and the calcination temperature employed here (773 K) is insufficient for the complete crystallization of the NiAl_2O_4 phase. But when the sample is heated further to 1073 K, the XRD pattern matches well with that of a nickel aluminate spinel structure (NiAl_2O_4 , JCPDS card no. 10-0339) in space group $Fd\bar{3}m$ with cubic symmetry and a lattice pa-

rameter $a = 0.8$ nm along with the presence of some minor NiO nanocrystals [asterisk (*) on the peak in the XRD pattern]. The particle size calculated by using the Scherrer equation from this wide-angle XRD pattern suggests a grain size of around 6 nm, which agrees well with electron-microscopic studies (see below). However, the main objective of our present study is to synthesize nickel–aluminum mixed-oxide material with maximum mesoporosity and a large surface area. Although the material heated at higher temperature (sample 4) exhibits better crystalline features, this material showed a very small surface area (see below). Indeed, the sample 3 (heated at 773 K) shows moderate crystalline features along with high porosity and large surface area, and this sample has shown better catalytic activity in the reduction of nitroarenes.

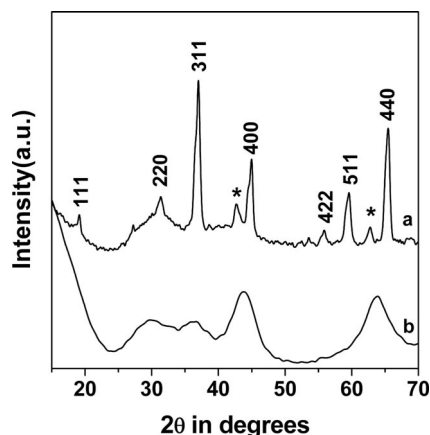


Figure 1. Wide-angle XRD pattern of mesoporous Ni–Al oxide samples 4 (a) and 3 (b).

N_2 -Sorption Measurement

Nitrogen adsorption/desorption isotherms of mesoporous nickel–aluminum oxide samples are shown in Figure 2. The Brunauer–Emmett–Teller (BET) surface area of sample 3 is $337 \text{ m}^2 \text{ g}^{-1}$, whereas sample 4, which calcined at 1073 K,

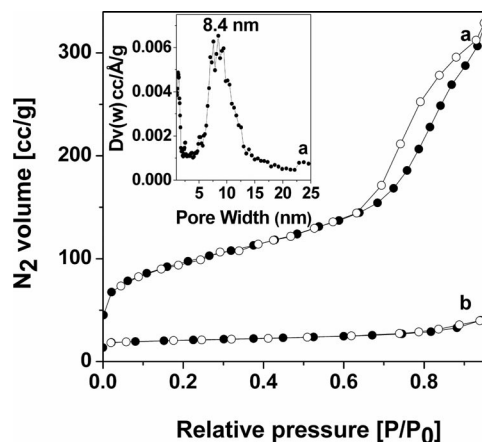


Figure 2. N_2 adsorption (●)/desorption (○) isotherms of samples 3 (a) and 4 (b) at 77 K. Pore-size distribution of sample 3 is shown in the inset.

shows a very small BET surface area of $21 \text{ m}^2 \text{ g}^{-1}$. From the difference of these data, it is clear that four repeating extractions followed by calcination at 773 K are able to remove the template lauric acid molecules and generate mesoporosity. But when this sample is heated to very high temperature (1073 K), the self-assembly of the NPs then collapses, and the material crystallizes completely into an NiAl_2O_4 spinel structure with no mesoporosity. Pore-size distribution (PSD) of sample **3** estimated by the nonlocal density functional theory (NLDFT; Figure 2, inset) suggests that the size of the pores is nearly 8.4 nm.

Nanostructure and Morphology

In Figure 3, TEM images of sample **3** are shown. From the TEM image (left) it is evident that the porosity of the material arises mainly from the interparticle separations. A close look at the image also reveals that the material is composed of many tiny close-packed particles of around 6–7 nm in size and that the particles are separated from each other at a distance of around 5–8 nm. It is possible that the template lauric acid molecules employed in the synthesis play the role of a capping agent, which restricts the particle-size growth. The high-resolution transmission electron microscopy (HRTEM) image (Figure 3, lower right) shows lattice fringes that correspond to (400) planes with a distance of 0.2 nm between two planes, which agrees well with the wide-angle d_{400} value of nickel aluminate spinel. The selected area electron diffraction (SAED) pattern (Figure 3, upper right) suggests that the wall of this mesoporous nickel–aluminum oxide is semicrystalline and composed of several (311), (400), and (440) planes of the nickel–alumininate spinel lattice crystal. Textural properties and particle size of the mesoporous material have been investigated by scanning electron microscopy (SEM) images. From Figure 4 we can see that the material is composed of tiny spherical particles, which self-assembled among themselves to form large clusters.

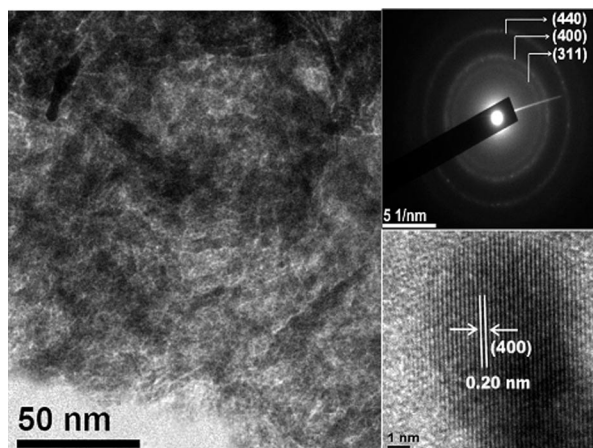


Figure 3. TEM image (left), HRTEM image showing the lattice fringes (lower right), and selected-area electron-diffraction pattern (upper right) of mesoporous $\text{NiO-Al}_2\text{O}_3$ sample **3**.

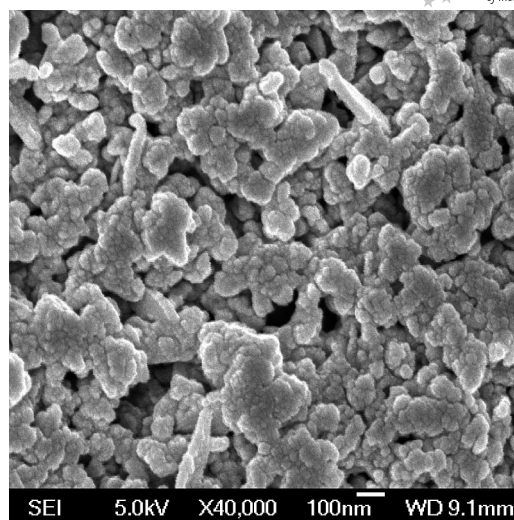


Figure 4. SEM image of the sample **3**.

Optical Study

UV/Vis spectroscopy can give us valuable information about the symmetry and coordination of the surface species of a catalyst. Figure 5 shows the UV/Vis spectra of sample **3**. The absorption is mainly due to ligand-to-metal charge-transfer transitions. The band observed near 396 nm could be attributed to the presence of octahedrally coordinated Ni^{2+} ($\text{O}^{2-} \rightarrow \text{Ni}^{2+}$ charge transfer), whereas the peaks observed in the vicinity of 681 and 738 nm could be attributed to the tetrahedral Ni^{2+} ions in this nickel–aluminum mixed-oxide material. For the bulk $\text{NiO}/\gamma\text{-Al}_2\text{O}_3$ samples with different Ni^{II} loadings, two absorption bands at 590 and 635 nm were attributed to tetrahedral Ni^{2+} ions, and a broad absorption band in the vicinity of 390 nm was attributed to octahedral Ni^{2+} .^[26] A moderate shift of the absorption bands from 390 to 396 nm and a very large shift of the 590 and 635 nm bands to 681 and 738 nm could be attributed to the surface-defect states^[27] that originated during hydrothermal synthesis in the presence of the capping agent, lauric acid molecules. As there is no sharp peak near 720 nm,^[28] we can conclude that NiO crystallites are not present at the $\text{NiO-Al}_2\text{O}_3$ surface, which also agrees well with the powder XRD result. It has been previously observed that when the nickel-ion loading is far below the dispersion capacity, the supported nickel ions preferentially incorporate into the tetrahedral vacancies of $\gamma\text{-Al}_2\text{O}_3$; and with increased nickel loading, the ratio of Ni^{2+} ions that incorporate into the octahedral vacancies of $\gamma\text{-Al}_2\text{O}_3$ increases.^[26] Since our mesoporous Ni-Al mixed-oxide material contains a very high concentration of Ni^{II} , both tetrahedral and octahedral coordination sites of Ni^{2+} are present in this material. NiAl_2O_4 is a largely inverse spinel that shows randomization of the distribution of Ni and Al atoms between the octahedral and tetrahedral cation sites in the framework with a change in temperature.^[29] This cation

distribution (and inversion degree) in the mesoporous Ni–Al mixed oxide can play a crucial role in its surface properties.

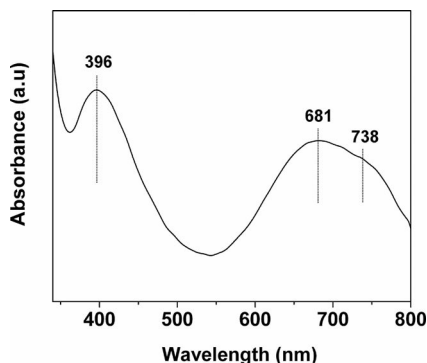


Figure 5. UV/Vis diffuse reflectance spectrum of mesoporous NiO–Al₂O₃ sample 3.

Metal–Template Interaction

FTIR spectra often give us information about metal–template interactions. In the FTIR spectra of the as-synthesized mesoporous Ni–Al mixed-oxide materials (not shown), two peaks are observed at around 2850 and 2922 cm⁻¹, which are assigned to the C–H stretching frequencies from the lauric acid molecules. These peaks are absent in sample 3, which indicates that, after heat treatment of the extracted sample, it is possible to remove the template completely, which also supports our sorption result. Long-chain fatty acid molecules are frequently used as capping agents to stabilize metal/metal oxide nanoparticles.^[30] The interaction between the precursor metal oxide species and the lauric acid molecules can be indirectly proved from the thermal analysis results. In Figure 6, the thermogravimetry (TG) and differential thermal analysis (DTA) plots for sample 1 are shown. The TG curve consists of three distinct weight losses. In the first step (i.e., in the temperature range 303–523 K), there is a weight loss of around 15%, which could be attributed to the removal of

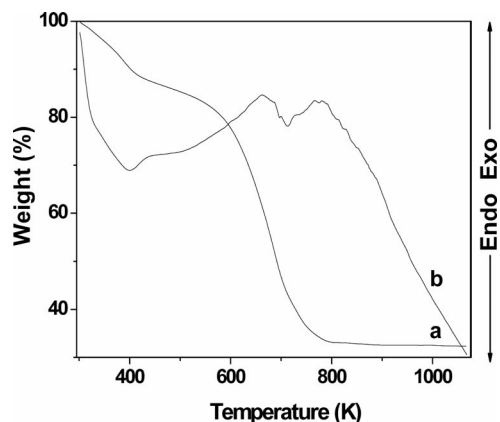


Figure 6. TG (a) and DTA (b) curves for as-synthesized sample 1.

the adsorbed water molecule from the surface. The second step (623–773 K) is related to a sharp weight loss of around 51%, thereby resulting in the removal of the organic capping agent (lauric acid) moiety from the material. A further weight loss of around 2.5% at 773–873 K associated with an exothermic peak in the DTA profile could be an indication of the transformation of mesoporous Ni–Al mixed oxide into an NiAl₂O₄ spinel structure.

Catalytic Hydride-Transfer Reduction

We carried out the liquid-phase hydride-transfer reaction with three different nitroarenes that contain activating and deactivating groups in the aromatic ring, and the results are summarized in Table 2. For all these nitroarenes, the mesoporous Ni–Al mixed-oxide catalyst 3 shows moderately good activity for the reduction of NO₂ groups. Selectivity for the reduction to the NH₂ group is exclusive in all the cases. For nitrobenzene, the conversion to aniline is 49.6%, whereas it is 57.8% for 4-chloronitrobenzene to 4-chloroaniline. A relatively low conversion (36.2%) has been achieved for *m*-dinitrobenzene to 3-nitroaniline by using this mesoporous nickel–aluminum oxide material. As seen from the table, the conversions of these nitroarenes follow the decreasing yield from the more activated aromatic ring of 4-chloronitrobenzene (+R effect) to the deactivated aromatic ring of *m*-dinitrobenzene. In all the cases, we can see that the catalyst is highly regioselective, and no further reduction of the benzene ring could occur. When the reaction is carried out in the absence of any catalyst, the reaction does not proceed at all (Table 2, Entry 4), thereby suggesting the catalytic role played by mesoporous Ni–Al mixed-oxide material. In the presence of pure alumina catalyst, the conversion is very low (Table 2, Entry 5), thereby suggesting that the presence of Ni^{II} at the active sites is mainly responsible for the above reduction reaction. Moreover, when the reaction was carried out by using catalyst 4 (high-temperature calcined sample) the product conversion comes down to only 28% (Table 2, Entry 6). This could be attributed to the fact that, after high-temperature calcination of the mesoporous Ni–Al mixed-oxide material, the porous framework collapses to a large extent. Hence the surface area diminishes and the amount of adsorbed reactant species does likewise.

In this hydride-transfer reduction reaction, nitroarenes are first adsorbed onto the surface of the catalyst. NaOH used in the reaction acts as a promoter to stabilize the adsorbed nitro groups present at the catalyst surface. Then the adsorbed nitroarene takes up hydrogen from the 2-propanol (it plays the role of hydride source) and forms a hydroxy-type intermediate, which further rearranges to a nitroso intermediate.^[31] This could be followed by two consecutive steps in which hydride transfer from 2-propanol^[32–35] to the nitroso and hydroxylamine species takes place to form the desired aniline. Ni^{II} sites present at the catalyst surface stabilize the 2-propanol molecules through adsorption and subsequent hydride transfer from the intermediate species.

Table 2. Liquid-phase catalytic reduction by using mesoporous Ni–Al mixed oxide.^[1]

Substrate	Reaction time [h]	Conversion [%]	Product
Nitrobenzene ^[a]	5	49.6	aniline
4-Chloro-1-nitrobenzene ^[a]	5	57.8	4-chloroaniline
<i>m</i> -Dinitrobenzene ^[a]	5	36.2	3-nitroaniline
Nitrobenzene ^[b]	6	0.4	aniline
4-Chloro-1-nitrobenzene ^[c]	6	0.6	4-chloroaniline
4-Chloro-1-nitrobenzene ^[d]	9	28.0	4-chloroaniline

[a] Reaction conditions: substrate (15 mmol), promoter (15 mmol), heated to reflux at 353 K in 2-propanol (15 mL), and sample 3 as catalyst (0.05 g cm³). [b] Reaction was carried out in the absence of catalyst. [c] Reaction was carried out by using pure alumina catalyst. [d] Reaction was carried out by using sample 4 (calcined at 1073 K).

In this way, the desired anilines are formed, which then desorb from the surface of the catalyst. Thus, the above results show that the surface Ni^{II} sites and the high BET surface area of our mesoporous nickel–aluminum oxide material are crucial in this catalytic hydride-transfer reduction reaction.

Conclusion

Mesoporous nickel–aluminum mixed-oxide material has been synthesized by a one-step hydrothermal route using lauric acid as the capping agent. The material showed a large surface area and high mesoporosity due to the interparticle separation assisted by the long-chain fatty acid molecules used during the hydrothermal synthesis. Liquid-phase hydride-transfer reactions were carried out for different nitroarenes by using this mesoporous mixed-metal oxide as catalyst and 2-propanol as hydride source under mild and environment-friendly conditions. The material showed moderately good catalytic activity in the reduction of nitroarenes together with high regioselectivity for the corresponding desired anilines.

Experimental Section

For the synthesis of mesoporous NiO–Al₂O₃ mixed-oxide, nickel chloride (NiCl₂, Merck) and aluminum chloride (AlCl₃, Merck) were used as the precursors for nickel and aluminum, respectively. Lauric acid (Merck) was used as capping agent. Nickel chloride (0.02 M) and aluminum chloride (0.02 M) were first dissolved in water (10 mL) and then blended with lauric acid (0.02 M, 20 mL) solution. The resulting mixture was stirred at 313 K for 2 h to obtain a clear sol. Ammonia solution was added dropwise to this solution until it formed a thick sky-blue precipitation. The pH of the mixture was maintained at around 10. The solution was hydrothermally treated at 373 K for 2 d, then filtered and thoroughly washed with water. To remove the capping agent, the as-synthesized material was treated four times with ethylenediamine/ethanol mixture at room temperature and finally calcined at 773 K in air for 2 h. The sample obtained after calcination at 773 K is designated as 3, the as-synthesized one as 1, and the fourth extracted one as 2. The sample calcined at 1073 K has been designated as sample 4. The molar composition of the synthesis mixture was 0.02 NiCl₂/0.02 AlCl₃/0.02 lauric acid.

Powder X-ray diffraction studies of different samples were carried out by using Ni-filtered Cu-K_α ($\lambda = 0.15406$ nm) radiation with a Bruker D-8 Avance diffractometer operated at 40 kV voltage and

40 mA current and calibrated with a standard silicon sample. Nitrogen adsorption–desorption isotherms were obtained with a Bel Japan Inc. Belsorp-HP instrument at 77 K. Samples were degassed at 423 K for 5 h prior to both the analyses. BET surface area and pore-size distribution were obtained according to the Brunauer–Emmett–Teller (BET) and NLDFT methods, respectively. For TEM analysis, a small amount of the powder sample was first dispersed in ethanol, and one drop of the dispersion was transferred onto a TEM Cu grid. It was allowed to dry in the ambient environment, and the analysis was carried out with a Jeol JEM 2010 transmission-electron microscope. The morphology of the sample was recorded by SEM (JEOL JEM 6700F with EDS attachment). UV/Vis diffuse reflectance spectra were obtained with a Shimadzu UV 2401PC spectrophotometer with an integrating sphere attachment by using a BaSO₄ pellet as background standard. FTIR spectra of these samples were recorded on KBr pellets with a Nicolet MAGNA-FT IR 750 series II spectrometer. Thermogravimetry (TG) studies and differential thermal analysis (DTA) were carried out with a TA Instruments SDT Q-600 thermal analyzer.

Liquid-phase hydride-transfer reactions were performed by using our various mesoporous NiO–Al₂O₃ mixed-oxide-based materials, namely, samples 3 (calcined at 773 K) and 4 (calcined at 1073 K). The reactions were also carried out with pure alumina and in the absence of any catalyst. Here we have chosen three different nitroarenes as substrate. The reactions were carried out in a two-necked round-bottomed flask fitted with a reflux condenser and temperature-controlled oil bath on a magnetic stirrer plate. In a typical reaction, the substrate (15 mmol) was mixed with NaOH (15 mmol; as promoter). Then 2-propanol (15 mL; it acts as solvent as well as reducing agent) and catalyst (0.05 g) were added to it. The temperature of the reaction was maintained at 353 K, and aliquots were collected at different time intervals. Finally, the catalyst was separated by filtration, and the products were analyzed with a gas chromatograph (Agilent 7890 A) equipped with a flame-ionization detector (FID) fitted with a capillary column.

Acknowledgments

A. B. wishes to thank the Department of Science and Technology (DST), New Delhi for financial support. M. P. and N. P. are grateful to the Council of Scientific and Industrial Research (CSIR), New Delhi for their senior research fellowships.

- [1] C. T. Kresge, M. E. Leonowicz, W. J. Roth, J. C. Vartuli, J. S. Beck, *Nature* **1992**, 359, 710–712.
 [2] a) J. Jimenez-Jimenez, P. Maireles-Torres, P. Olivera-Postor, E. Rodriguez-Castellon, A. Jimenez-Lopez, D. J. Jones, J. Roziere, *Adv. Mater.* **1998**, 10, 812–815; b) B. Z. Tian, X. Y. Liu, B. Tu, C. Z. Yu, J. Fan, L. M. Wang, S. H. Xie, G. D. Stucky, D. Y. Zhao, *Nat. Mater.* **2003**, 2, 159–163; c) K. Sarkar, T. Yokoi, T.

- Tatsumi, A. Bhaumik, *Microporous Mesoporous Mater.* **2008**, *110*, 405–412.
- [3] a) X. He, D. Antonelli, *Angew. Chem. Int. Ed.* **2002**, *41*, 214–229; b) T.-Y. Ma, Z.-Y. Yuan, J.-L. Cao, *Eur. J. Inorg. Chem.* **2010**, 716–724.
- [4] a) S. Inagaki, S. Guan, Y. Fukushima, T. Ohsuna, O. Terasaki, *J. Am. Chem. Soc.* **1999**, *121*, 9611; b) T. Asefa, M. J. MacLachlan, N. Coombs, G. A. Ozin, *Nature* **1999**, *402*, 867; c) A. Bhaumik, M. P. Kapoor, S. Inagaki, *Chem. Commun.* **2003**, 470–471; d) J. A. Melero, R. van Grieken, G. Morales, *Chem. Rev.* **2006**, *106*; e) D. Chandra, A. Dutta, A. Bhaumik, *Eur. J. Inorg. Chem.* **2009**, 4062–4068; f) J. M. Kim, C. H. Shin, R. Ryoo, *Catal. Today* **1997**, *38*, 221–226.
- [5] Y. Wang, J. Ren, Y. Wang, F. Zhang, X. Liu, Y. Guo, G. Lu, *J. Phys. Chem. C* **2008**, *112*, 15293–15298.
- [6] J.-Y. Luo, Y.-G. Wang, H.-M. Xiong, Y.-Y. Xia, *Chem. Mater.* **2007**, *19*, 4791–4795.
- [7] Y. Tang, L. Yang, Z. Qiu, J. Huang, *J. Mater. Chem.* **2009**, *19*, 5980–5984.
- [8] M. A. Carreon, V. V. Gulians, *Eur. J. Inorg. Chem.* **2005**, 27–43.
- [9] a) J. C. Arrebola, A. Caballero, L. Hernan, J. Morales, *Eur. J. Inorg. Chem.* **2008**, 3295–3302; b) Y.-K. Sun, D. H. Kim, C. S. Yoon, S.-T. Myung, J. Prakash, K. Amine, *Adv. Funct. Mater.* **2010**, *20*, 485–491.
- [10] N. Guilhaume, M. Primet, *J. Chem. Soc. Faraday Trans.* **1994**, *90*, 1541–1545.
- [11] T.-Y. Ma, Z. Y. Yuan, J. L. Cao, *Eur. J. Inorg. Chem.* **2010**, 716–724.
- [12] K.-T. Li, M.-Y. Huang, W.-D. Cheng, *Ind. Eng. Chem. Res.* **1996**, *35*, 621–626.
- [13] K.-T. Li, C.-H. Huang, *Can. J. Chem. Eng.* **1999**, *77*, 1141–1145.
- [14] N. S. Chaubal, M. R. Sawant, *J. Mol. Catal. A* **2007**, *261*, 232–241.
- [15] Y. Cesteros, P. Salagre, F. Medina, J. E. Sueiras, *Chem. Mater.* **2000**, *12*, 331–335.
- [16] X. Xiang, H. I. Hima, H. Wang, F. Li, *Chem. Mater.* **2008**, *20*, 1173–1182.
- [17] a) C. O. Areán, M. P. Mentrui, A. J. López López, J. B. Parra, *Colloids Surf., A* **2001**, *180*, 253–258; b) P. Kim, Y. Kim, H. Kim, I. K. Song, J. Yi, *Appl. Catal. A* **2004**, *272*, 157–166.
- [18] G. Tai, W. Guo, *Mater. Chem. Phys.* **2007**, *103*, 201–205.
- [19] L. M. Bronstein, M. Kostylev, E. Shtykova, T. Vlahu, X. Huang, B. D. Stein, A. Bykov, N. B. Remmes, D. V. Baxter, D. I. Svergun, *Langmuir* **2008**, *24*, 12618–12626.
- [20] a) T. Ishida, M. Haruta, *Angew. Chem. Int. Ed.* **2007**, *46*, 7154–7156; b) A. Corma, H. Garcia, *Chem. Soc. Rev.* **2008**, *37*, 2096–2126; c) S. Elzey, A. Mubayi, S. C. Larsen, V. H. Grassian, *J. Mol. Catal. A* **2008**, *285*, 48–57; d) M. Paul, N. Pal, B. S. Rana, A. K. Sinha, A. Bhaumik, *Catal. Commun.* **2009**, *10*, 2041–2045; e) T. C. Nagaiah, A. Maljusch, X. X. Chen, M. Bron, W. Schuhmann, *ChemPhysChem* **2009**, *10*, 2711–2718.
- [21] H. Mahadevi, B. Tamami, *Synth. Commun.* **2005**, *35*, 1121.
- [22] F. A. Khan, J. Dash, C. Sudheer, R. K. Gupta, *Tetrahedron Lett.* **2003**, *44*, 7783.
- [23] D. Nagaraja, M. A. Pasha, *Tetrahedron Lett.* **1999**, *40*, 7855.
- [24] P. Kim, Y. Kim, H. Kim, I. K. Song, J. Yi, *J. Mol. Catal. A* **2004**, *219*, 87.
- [25] M. H. Zahir, K. Sato, H. Mori, Y. Iwamoto, *J. Am. Ceram. Soc.* **2006**, *89*, 2874–2880.
- [26] R. Shibiao, Q. Jinheng, W. Chunyan, X. Bolian, F. Yining, C. Yi, *Chin. J. Catal.* **2007**, *28*, 651–656.
- [27] K. D. Becker, F. Rau, *Ber. Bunsen-Ges. Phys. Chem.* **1992**, *96*, 1017–1027.
- [28] F. Romero-Sarria, J. C. Vargas, A. C. Roger, A. Kiennemann, *Catal. Today* **2008**, *133–135*, 149–153.
- [29] a) H. S. O'Neill, W. A. Dollase, C. R. Ross, *Phys. Chem. Miner.* **1991**, *18*, 302–319; b) J. A. Azurdia, J. Marchal, P. Shea, H. P. Sun, X. Q. Pan, R. M. Laine, *Chem. Mater.* **2006**, *18*, 731–739; c) I. Prakash, P. Muralidharan, N. Nallamuthu, N. Satyanarayana, M. Venkateswarlu, D. Carnahan, *J. Am. Ceram. Soc.* **2006**, *89*, 2220–2226.
- [30] a) Y. Wang, H. Yang, *Chem. Commun.* **2006**, 2545–2547; b) C. L. Wang, H. Zhang, J. H. Zhang, M. J. Li, K. Han, B. Yang, *J. Colloid Interface Sci.* **2006**, *294*, 104–108.
- [31] a) X. Meng, H. Cheng, Y. Akiyama, Y. Hao, W. Qiao, Y. Yu, F. Zhao, S.-i. Fujita, M. Arai, *J. Catal.* **2009**, *264*, 1–10; b) P. Forzatti, I. Nova, E. Tronconi, *Angew. Chem. Int. Ed.* **2009**, *48*, 8366–8368.
- [32] R. A. W. Johnstone, A. H. Wilby, I. D. Entwistle, *Chem. Rev.* **1985**, *85*, 129–170.
- [33] K. Yamaguchi, T. Koike, M. Kotani, M. Matsushita, S. Shinachi, N. Mizuno, *Chem. Eur. J.* **2005**, *11*, 6574–6582.
- [34] W. Baratta, P. Rigo, *Eur. J. Inorg. Chem.* **2008**, *26*, 4041–4053.
- [35] C. A. Sandoval, Y. H. Li, K. L. Ding, R. Noyori, *Chem. Asian J.* **2008**, *3*, 1801–1810.

Received: July 5, 2010

Published Online: September 29, 2010